Tailoring Metaheuristics for Designing Thermodynamic-Optimal Cooling Devices for Microelectronic Thermal Management Applications

Guillermo Pérez-Espinosa, Jorge M. Cruz-Duarte, Ivan Amaya,
José C. Ortiz-Bayliss, Hugo Terashima-Marín
School of Engineering and Science, *Tecnologico de Monterrey*
Monterrey, Mexico
Emails: {A01172974, jorge.cruz, jcobayliss, iamaya2, terashima}@tec.mx

Nelishia Pillay
Department of Computer Sciences,
University of Pretoria
Pretoria, South Africa
Email: npillay@cs.up.ac.za

***Abstract*—Heat sinks are a prevalent and direct solution for addressing the Microelectronic Thermal Management Problem (MTMP), which is critical in today's electronic industry. Specifically, an optimally designed thermodynamic heat sink ensures that microelectronics operate reliably without compromising their lifespan and performance, thereby indirectly safeguarding user safety. Although Metaheuristics (MHs) have proven effective in tackling this complex design challenge due to their robust characteristics, no single MH consistently delivers superior performance across all scenarios. The study explores the feasibility of an Automated Metaheuristic Design strategy, employing a hyper-heuristic search to develop a population-based, metaphor-free MH specifically for the MTMP. Various scenarios are assessed by varying the heat sink design specifications and benchmarking the custom MH designs against several state-of-the-art MHs. The findings of this preliminary work provide statistical evidence that the tailored MHs surpass the performance of established MHs in these scenarios. A toolkit of MH components is assembled, which can be customized to construct MHs specifically for MTMPs. This approach enables practitioners to select the most suitable solver for a particular problem without needing extensive expertise in heuristic-based optimization.**

***Index Terms*—Parameter Tuning and Algorithm Configuration, Electronic Thermal Management, Microchannel Heat Sinks, Metaheuristics, Heuristics, Evolutionary Algorithms.**

I. Introduction

Thermal management has become increasingly critical in recent years due to the ongoing miniaturization and demand for higher performance in electronic components. As these components grow more compact and powerful, they generate more heat, jeopardizing their performance and structural integrity. Therefore, effective cooling techniques are essential in developing new, high-performance devices. Among various cooling solutions, heat sinks stand out as a prevalent choice. They are favored for their direct manufacturing process, cost-effectiveness, and efficient heat dissipation capabilities [1]. Heat sink designs can vary significantly, with choices in base materials, coolant types, and geometric configuration all influencing performance [2]. Consequently, designing heat sinks presents a practical optimization challenge, where design variables constitute the search space and metrics such as entropy generation serve as cost functions [3], [4].

Various optimization methodologies have been explored, each exhibiting unique strengths and limitations. Metaheuristics (MHs) have gained prominence due to their reliability, flexibility, and straightforward implementation. These qualities have made MHs increasingly popular for solving complex optimization problems across diverse fields. The literature offers a plethora of MHs, allowing practitioners to select an approach tailored to specific needs. However, a significant challenge arises from the inherent limitations of MHs, encapsulated by the No-Free-Lunch theorem, which suggests that no single algorithm consistently outperforms others across all problems [5]. Despite claims of superiority in diverse engineering applications [6]–[8], selecting an optimal MH for a particular scenario remains a non-trivial task. Effective selection requires deep knowledge of the available MHs, including how to tune parameters and adjust settings to optimize performance for specific tasks. This need for expertise highlights a critical abstraction challenge: choosing the most suitable MH for a given optimization problem.

The above-mentioned is called the Metaheuristic Composition Optimization Problem (MCOP). Addressing this challenge requires a high-level solver capable of navigating through a set of available MHs to identify the most suitable one for a given context. Such solvers are Hyper-Heuristics (HHs), which function as advanced search strategies. Recently, HHs have been effectively employed to tackle combinatorial [9] and continuous optimization problems [10]. Among the significant contributions in this area is the CUSTOMHyS framework, as described in [10]. This framework allows for generating MHs by selecting from a diverse set of Search Operators (SOs). It offers the flexibility to adjust parameters according to user requirements. Claims from the authors suggest that MHs generated by CUSTOMHyS outperformed both handcrafted and "bio-inspired" MHs. The potential of this approach offers a compelling alternative to conventional methods. However, the effectiveness of tailored MHs hinges crucially on the selection of operators. A well-curated pool of operators, aptly suited for the problem across various scenarios, ensures that the developed MHs perform robustly and adapt more effectively

in each HH implementation. Thus, these operators' strategic selection and application enable a more flexible and potent solution strategy, maximizing performance across diverse and potentially more complex scenarios.

This work introduces an HH approach that utilizes the CUSTOMHyS framework to address the Microelectronic Thermal Management Problem (MTMP). We have developed a mathematical model to simulate entropy generation within a rectangular microchannel heat sink, which serves to assess the efficacy of each tailored MH. The main focus of this work is to find a procedure for identifying search operators that work well in this problem domain; comparing the tailored MHs with top-notch metaheuristics is outside the scope. So, this research encompasses three experimental sets using four different base materials and one coolant type. In each experimental set, we systematically alter the selection of operators, evaluating and contrasting the performance of the resulting reduced collection of operators with that of the baseline set. Statistical analysis confirms that the MHs configured with the curated operator collection outperform those assembled from the default collection, demonstrating enhanced efficiency and effectiveness.

II. Theoretical Foundations

This section briefly describes several essential concepts related to the automated algorithm design, particularly metaheuristics and the microchannel heat sink design.

A. Automated Metaheuristic Design

The Automated Algorithm Design (AAD) about MHs solving continuous optimization problems is often defined as the MCOP [11], a variant of the General Combinatorial Optimization Problem [12]. Therefore, a technique that solves the MCOP given by

$$(\mathrm{MH}_*; \vec{x}_*) = \underset{\mathrm{MH}\in\mathfrak{H},\, \vec{x}\in\mathfrak{X}}{\operatorname{argmax}} \{Q(\mathrm{MH}\,|\mathfrak{X})\} \tag{1}$$

corresponds to a high-level algorithm, namely a Hyper-Heuristic, no matter its nature, because it searches within a portion of the heuristic space $\mathfrak{H} \subseteq \mathbb{H}^{\varpi}$ to find the best heuristic sequence that composes the optimal metaheuristic (MH_*) rendering a maximal performance $Q(\mathrm{MH}_*\,|\mathfrak{X})$ [13]. (ϖ represents the number of SOs in the MH.) Such an MH_*, representing the optimal solver at a low-level abstraction, addresses a specific problem $(\mathfrak{X}, f)$ or a related family of problems to attain the optimal solution $\vec{x}_*$ within the feasible domain $\mathfrak{X}$. While a detailed discussion of these terms is available in the existing literature [14], [15], we briefly introduce several pertinent terms below.

Initially, a general optimization problem is defined on a feasible domain $\mathfrak{X} \subseteq \mathfrak{S}$, since $\mathfrak{S}$ represents any arbitrary domain. The goal is to minimize (or maximize) a real-valued objective function $f(\vec{x})$, where $\vec{x} \in \mathfrak{X}$ maps to $\mathbb{R}$. The problem $(\mathfrak{X}, f)$ can be expressed as follows,

$$\vec{x}_* = \underset{\vec{x}\in\mathfrak{X}}{\operatorname{argmin}} \{f(\vec{x})\}, \tag{2}$$

where $\vec{x}_* \in \mathfrak{X}$ minimizes f within $\mathfrak{X}$. We define the feasible domain as a general representation of any domain bounded by arbitrary constraints, which can be simple or complex depending on the application [11]. Additionally, we consider the level of abstraction, allowing $\mathfrak{S}$ to represent the general heuristic space at a high level. Consequently, MCOP stands for a specific instance of the minimization problem described in (2), where $\mathfrak{X} \subset \mathfrak{H}^{\varpi}$ and employs the duality principle. At a lower level of abstraction, problems pertinent to thermodynamic design manifest as continuous real-valued minimization tasks, hence $\mathfrak{X} \subset \mathbb{R}^D$. Here, D denotes the number of design variables, and f relates to the entropy generation rate. These two problem domains are detailed below.

B. Heuristics: High-Level Problem Domain

A heuristic is defined as a procedure that either directly or indirectly generates or modifies candidate solutions for a specific problem [14]. Terms like heuristic and metaheuristic are often used interchangeably, leading to confusion, especially when including hyper-heuristics in the equation. We adopt the general definition in [11] and categorize heuristics into three types based on their interaction with the problem domain: Simple Heuristics (SHs), Metaheuristics (MHs), and Hyper-Heuristics (HHs) [15], [16]. Depending on that interaction, SHs are classified as:

- *Constructive* heuristics that build candidates from scratch;
- *Perturbative* heuristics that modify candidates using insights from the solving process and problem context; and
- *Selective* heuristics that assess and decide on candidates.

In practice, a selective heuristic often follows a perturbative heuristic, forming well-defined SOs, such as combining the Local Random Walk perturbator and Metropolis selector in Simulated Annealing.

Metaheuristics are positioned at a mid-level because they interface with the problem domain by orchestrating an iterative process involving SHs [8]. An MH is characterized by three essential components: an initializer (or a constructive heuristic) h_i, at least one search operator h_o, and a finalizer (or a selective heuristic) h_f [15]. Notably, the *finalizer* was not previously introduced as it operates at a higher level as part of what is so-called the *master strategy* [15]. Therefore, we represent an MH as $\mathrm{MH} = \langle h_i, h_o, h_f \rangle$. Here, h_o may consist of multiple SOs arranged sequentially, i.e., $h_o = h_{\varpi} \circ \cdots \circ h_1$, where each $h_k \in \vec{h} \in \mathfrak{H}$. Given the non-commutative nature of SOs, and for clarity, h_o is composed application-wise. For a more precise representation, we denote the reversed composition as $\bar{h}_o$, which is easier to understand.

Lastly, HHs are high-level heuristics that indirectly interact with the problem domain by exploring the heuristic space to find a SHs sequence for computing solutions [17]. The critical difference between an MH and an HH is their operational approach: MHs follow a predetermined sequence or procedure to generate a solution, whereas HHs autonomously reorganize to optimize the arrangement of operators for effectively solving a specific problem [16].

C. Low-Level Domain: Microelectronic Thermal Management

The Microelectronic Thermal Management Problem (MTMP) is a highly relevant topic nowadays [18]. In many applications, the primary objective is to prevent overheating of electronic and electromechanical components within devices, as overheating significantly reduces their lifespan and performance. Approximately 55% of electronic device failures are attributed to high temperatures and inadequate heat dissipation [18]. To combat this, various solutions have been proposed in microelectronic manufacturing, with Microchannel Heat Sinks (MCHSs) emerging as a prevalent option. MCHSs are favored for their ability to manage the intense thermal fluxes associated with Very Large Scale Integration (VLSI) technology and modern System on a Chip (SoC) architectures, which incorporate CPUs, memories, GPUs, I/O interfaces, among others [19]. Figure 1 presents a conceptual scheme of a rectangular MCHS, detailing its thermal interface, the chip, and the fluid flow supply tubes for illustration purposes [20]. The following lines briefly explain how the MCHS works and which equations govern its behavior.

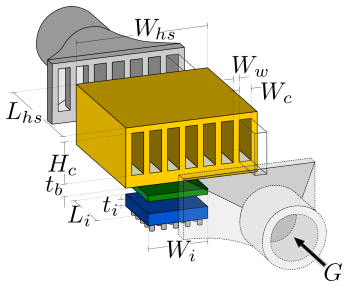

Fig. 1. Conceptual illustration of a rectangular microchannel heat sink in yellow, its thermal interface in green, an arbitrary microelectronic device in blue, and two fluid flow supply tubes in gray.

First, the geometry of the MCHS is depicted in Fig. 1, showing the principal dimensions. The total volume of the MCHS, excluding fluid, is calculated as $W_{hs}L_{hs}(H_c + t_t + t_b)$ [m^3], where t_t [m] and t_b [m] represent the thicknesses of the upper and lower parallel plates, respectively, enclosing the plate fin array. The number of microchannels, determined by the spaces between plate fins, is calculated as $N_c = (W_{hs} - W_w)/(W_c + W_w)$, where each channel has a width of W_c [m], a height of H_c [m], a length of L_{hs} [m], and a wall thickness of W_w [m] (see Fig. 1). Additionally, the coolant flowing through these channels has a volume flow rate of G [m^3/s], and its volume within the MCHS is $N_c H_c W_c L_{hs}$. The interface's effective heat transfer area from the chip is calculated by $A_i = W_i L_i$ [m^2], and $\dot{q}$ [W/m^2] represents the heat flux generated by the electronic device. Certain assumptions about heat transfer and fluid mechanics, which are not detailed here for brevity, ground our model. These assumptions are based on the works cited [21]–[23], which employed similar conditions.

Several approaches exist to describe MCHS behavior. This work employs thermodynamic modeling using the Entropy Generation Minimization (EGM) criterion [21], [24]. Given the details discussed previously, the entropy generation model for the system shown in Fig. 1 is represented by

$$\dot{S}_{\text{gen}} = \frac{\dot{Q}^2}{T_a T_i} R_{\text{eq}} + \frac{G_d}{T_a} \Delta P, \tag{3}$$

since $\dot{S}_{\text{gen}}$ [W/K] denotes the total entropy generation rate during the operation of the system [21]. This rate is the cost function for designing the MCHS design under the second law of thermodynamics. The r.h.s. terms of (3) represent entropy production due to heat transfer and fluid flow irreversibilities, respectively. These measurements indicate the degree to which the system deviates from ideal behavior. Further, in (3), $\dot{Q}$ [W] is the net power dissipated by the chip, R_{eq} [K/W] is the equivalent thermal resistance of the MCHS, T_a [K] and T_i [K] are the surrounding and chip temperatures, respectively, G_d [m^3/s] is the net volume flow rate of the coolant, and ΔP [Pa] is the total pressure drop necessary to maintain coolant flow [25]. Below, we explore two crucial components, R_{eq} and ΔP, which present a clear trade-off. Governed by the EGM criterion, these guide us to the thermodynamically optimal and typically more eco-friendly solution.

In this work, we focus on the MCHS's equivalent thermal resistance represented by the solid structure and the fluid within the microchannels as given by [22],

$$R_{\text{eq}} = \frac{m}{\bar{h} N_c L_{hs} (m W_c + 2 \tanh(m H_c))} + \frac{1}{\rho_f c_f G}. \tag{4}$$

The first and second r.h.s. terms correspond to the resistances due to convection in the microchannels and the calorific capacity of the working fluid, respectively. The convective resistance involves parameters like N_c, as well as the average film coefficient $\bar{h}$ [W/m^2·K], and the dimensionless fin parameter m [21], [25]. The film coefficient $\bar{h}$ is estimated from $\bar{h} = \text{Nu} k_f / D_h$, where Nu is the Nusselt number, k_f [W/m·K] represents the fluid's thermal conductivity, and D_h [m] the hydraulic diameter [26]. The fluid thermal resistance, the second r.h.s. term in (4), depends on the fluid's average density ρ_f [kg/m^3] and specific heat c_f [J/kg·K], and the volume flow rate G [m^3/s].

Similarly, to determine the entropy production from the mass transfer, the total pressure drop ΔP [Pa] across the system is calculated as follows [26],

$$\Delta P = \frac{\rho_f \bar{V}_f^2}{2} \left(f \frac{L_{hs}}{D_h} + 1.79 - 2.32\hat{\beta} + 0.53\hat{\beta}^2 \right) \tag{5}$$

since $\hat{\beta} = \beta/(1+\beta)$, $\bar{V}_f$ [m/s] is the average fluid velocity, $\beta = W_c/W_w$ is the channel wall aspect ratio, and f is the Darcy friction factor [21], [22].

In accordance with the operating conditions from [21]–[23], we considered empirical correlations for the Nusselt number Nu and the friction factor f, which depend on the channel aspect ratio $\alpha = W_c/H_c$ and the fluid's kinematic viscosity ν_f [m^2/s] [22]. These correlations are valid under specific flow regimes: laminar for Re < 2300 and turbulent for Re > 2300, with the transitional regime not considered.

III. Methodology

This work employs an AAD strategy to tailor MHs with similar or better performance than several state-of-the-art MHs. Furthermore, we distilled the heuristic space to identify SOs that best suit this application. Ultimately, we looked to improve the overall AAD procedure for designing MHs for MCHS applications. We used the CUSTOMHyS framework to ease the implementation of the proposed approach. This framework is freely available at https://pypi.org/project/customhys/ [27], and it was accessed on June 19th, 2023. Moreover, all data this work achieved is freely available at https://github.com/GuillermoPerezE/Microchannels. CUSTOMHyS uses population-based SOs found in the literature to tailor new MHs. The maximum length of this new MH can be determined, allowing for a vast number of potential MHs in the search space, limited only by the size of the collection used in experimentation.

Initially, we selected materials for constructing the MCHS, including Copper (Cu), High Thermal Conductive Graphite (HTCG), Aluminum (Al), and Silicon (Si), applicable across various manufacturing processes. Water (H_2O) was chosen as the coolant due to its abundance and ease of use. Although combining Copper with Water presents certain practical challenges, this study does not consider these. These considerations were made for illustrative purposes. Table I lists the relevant thermophysical properties of each material and fluid. Additionally, Table II outlines the design conditions for the MCHS, while Table III details the simple constraints defining the feasible design region.

TABLE I
THERMOPHYSICAL PROPERTIES OF THE CONSIDERED MATERIALS AND WORKING FLUID TO DESIGN MICROCHANNEL HEAT SINKS.

Material/Fluid	ρ [kg/m^2]	k [W/m·K]	ν [m^2/s]	c [J/kg·K]
Aluminum (Al)	2707	237	-	900
Copper (Cu)	8954	401	-	376.812
Graphite (HTCG)	1000	1900	-	742
Silicon (Si)	2330	148	-	700
Water (H_2O)	994.2	0.6250	7.29×10^{-7}	4178

TABLE II
PARAMETER VALUES CORRESPONDING TO THE DESIGN CONDITION OF A MICROCHANNEL HEAT SINK.

Parameter(s)	L_{hs}, L_i	W_{hs}, W_i	H_c	t_b	$\dot{q}$
Value	51 mm	51 mm	1.7 mm	0.1 mm	150 kW/m^2

The experimentation process was divided into three parts, conducted using four different material instances and various configurations of the HH, detailed in Table IV. The default configuration is based on CUSTOMHyS, with the other four configurations altering only one parameter from the default at a time. Plus, Table V displays the initial collection of SOs, comprising 12 families, each containing varying numbers of members.

TABLE III
SIMPLE CONSTRAINTS THAT GIVE PLACE TO THE FEASIBLE REGION IN THE DESIGN PROBLEM OF A MICROCHANNEL HEAT SINK.

Parameter	α	β	G_d [m^3/s]
Lower Boundary	0.001	2	0.001
Upper Boundary	1	1000	10^{-6}

TABLE IV
HYPER-HEURISTIC PARAMETER CONFIGURATIONS CONSIDERED FOR THE EXPERIMENTS. WE USED 30 REPLICAS AND 100 STEPS.

Exp. Conf.	Cardinality	Iterations	Agents	Stagnation (%)
Default	3	30	100	30
Config 1	3	50	100	30
Config 2	2	30	100	30
Config 3	3	50	30	30
Config 4	3	30	100	10

TABLE V
DEFAULT COLLECTION OF SEARCH OPERATORS FROM CUSTOMHYS GROUPED BY FAMILIES. NOS: NUMBER OF OPERATORS.

Family	NOs	Family	NOs
Random Search	13	Central Force Dynamic	4
Differential Mutation	24	Firefly Dynamic	12
Genetic Crossover	80	Genetic Mutation	12
Gravitational Search	4	Random Flight	12
Local Random Walk	12	Random Sample	4
Spiral Dynamic	4	Swarm Dynamic	24

We employed a three-fold methodology for our experiments. Initially, the HH was executed 30 times for each of the four material combinations: Al-H_2O, Cu-H_2O, Si-H_2O, and HTCG-H_2O, focusing mainly on the Aluminum and Water combination. The most effective MH in this scenario was selected for further analysis. This selected MH was then compared against seven well-known state-of-the-art MHs, including Random Search (RS), Simulated Annealing (SA), Genetic Algorithms (GA), Differential Evolution (DE), Particle Swarm Optimization (PSO), Cuckoo Search (CS), and a Hybrid MH with Swarm Dynamic and Genetic Crossover operators [27]. Each MH was run for 100 iterations and 30 repetitions per material combination for a comprehensive evaluation. The statistical significance of performance improvements was assessed using the one-sided Wilcoxon signed-rank test.

In the second phase of the experimentation, we refined the initial operator collection by selecting SOs from the best-performing MHs across each configuration and material combination, thereby creating a new collection. The HH then ran with the new collection. Following the established selection procedure, one MH from the Al+H_2O combination was chosen for further evaluation. This new MH was compared against the previously tailored MH using the same statistical testing method to assess significant performance improvements.

In the third and final phase of our experimentation, we refined the operator collection further by retaining only the 14 most frequently used operators from the second phase. The HH

was run with this new collection. A final MH from the Al+H_2O combination was selected and evaluated against the tailored MHs from the first two phases using the same statistical testing to assess any performance improvements. This step aimed to compare the performance enhancements across three different heuristic spaces under consistent conditions.

Moreover, the mathematical model outlined in Section II was implemented using Python 3.9. The experiments were conducted on a system with 2x Intel Xeon Gold 5122 Processors @ 3.6 GHz (16 logical CPUs), 128 GB RAM, and 1x Tesla V100-PCIE 32 GB GPU RAM.

IV. Results

The box plots in the subsequent figures offer a visual analysis of extensive data, simplifying interpretation. Fig. 2 illustrates the metric values' distribution from the initial experimental series, conducted with material and configuration pairings detailed in Table IV. Each configuration's value distribution varied, with the fourth configuration yielding the least favorable results and the first showing the most consistently high performance. These outcomes align with expectations, given that these particular configurations significantly influence the duration of the search process, where longer searches typically yield more precise results. Notably, material selection impacts entropy generation, as evidenced by HTCG and Copper, which consistently results in lower entropy generation values.

First, a curated collection was assembled by selecting the most effective MH from each configuration for every material combination. These MHs were then broken down into their constituent SOs, forming Collection 1, detailed in Table VI. This process significantly reduced the collection size from 205 to 33 operators, eliminating certain operator families and leaving others with a single operator, risking their exclusion in subsequent curation. However, three families stood out, indicating their effectiveness and hinting at their probable retention in future collections.

TABLE VI
Collection 1 of search operators grouped by families and heuristic identifier (h_k).

Family	Number of Operators	$\bar{h}_k$
Random Search	2	$\bar{h}_0, \bar{h}_{24}$
Central Force Dynamic	1	$\bar{h}_1$
Differential Mutation	7	$\bar{h}_2, \ldots, \bar{h}_8$
Firefly Dynamic	1	$\bar{h}_9$
Genetic Crossover	11	$\bar{h}_{10}, \ldots, \bar{h}_{20}$
Genetic Mutation	1	$\bar{h}_{21}$
Random Flight	1	$\bar{h}_{22}$
Local Random Walk	1	$\bar{h}_{23}$
Swarm Dynamic	8	$\bar{h}_{25}, \ldots, \bar{h}_{32}$

The HH was executed using the newly curated collection. Performance outcomes for the tailored MHs, depicted in Fig. 3, indicate an improvement with Collection 1, in terms of better average performance and consistency, compared to those shown in Fig. 2. The results reaffirm that Copper (Cu) and High Thermal Conductive Graphite (HTCG) are superior materials for the design, and Configuration 1 consistently yields the best-performing MHs.

For the final iteration of collection curation, we distilled the set down to the 14 operators most frequently utilized in the tailored MHs, as evidenced by Fig. 3. The frequency distribution of these operators within Collection 1 is illustrated in Fig. 4, where it is clear that while each operator was used at least once, a subset emerged as particularly efficacious, recurring more frequently across tailored MHs. This prevalence suggests their superior capability to address the problem effectively. These select 14 SOs, now encapsulated as Collection 2, are listed in Table VII. In line with prior observations, this collection retains the three standout operator families from Collection 1, emphasizing their continued relevance and efficacy.

TABLE VII
Collection 2 of search operators given by a Perturbator, with its most relevant parameters, and a Selector (Greedy, Probabilistic, and Metropolis).

$\bar{h}_k$	Perturbator	Parameters	Selector
$\bar{h}_0$	Differential Mutation	`/random/1/`	Greedy
$\bar{h}_1$		`/best/`	Probabilistic
$\bar{h}_2$		`/current/`	Greedy
$\bar{h}_3$		`/current-to-best/`	Greedy
$\bar{h}_4$		`/random-to-best/`	Greedy
$\bar{h}_5$		`/random-to-best-and-current/`	Greedy
$\bar{h}_6$	Genetic Crossover	Rank Pairing, Blend Crossover	Greedy
$\bar{h}_7$			Metropolis
$\bar{h}_8$			Probabilistic
$\bar{h}_9$	Swarm Dynamic	Inertial, Gaussian Distribution	Greedy
$\bar{h}_{10}$		Constricted, Uniform Distribution	Metropolis
$\bar{h}_{11}$			Probabilistic
$\bar{h}_{12}$		Constricted, Gaussian Distribution	Greedy
$\bar{h}_{13}$			Probabilistic

The automated algorithm design procedure using Simulated Annealing as a hyper-heuristic was run one last time using Collection 2. Figure 5 displays the performance of the resulting MHs, revealing marked improvements in efficacy and consistency. The initial observation is an improvement in both the implementation and consistency of these MHs. For instance, the results using Config 1 for the Copper, Silicon, and HTCG material variations achieve such high-performance levels that variations are negligible. Config 1 consistently delivers the best results across all scenarios. Yet, Figure 5 reveals a notable enhancement in the performance of Config 4, rendering it comparable to the other configurations under certain conditions. This improvement is specific to the curated collection. It suggests that Config 4 may be a viable alternative due to its time and resource efficiency despite slightly lagging behind other configurations in results. The advantage of Config 4 lies in its ability to reduce the exploration time of the HH by minimizing stagnation percentages.

Further analysis of the MHs tailored from this collection, which exhibited superior performance, revealed a shared feature: the most successful MHs incorporated three SOs, begin-

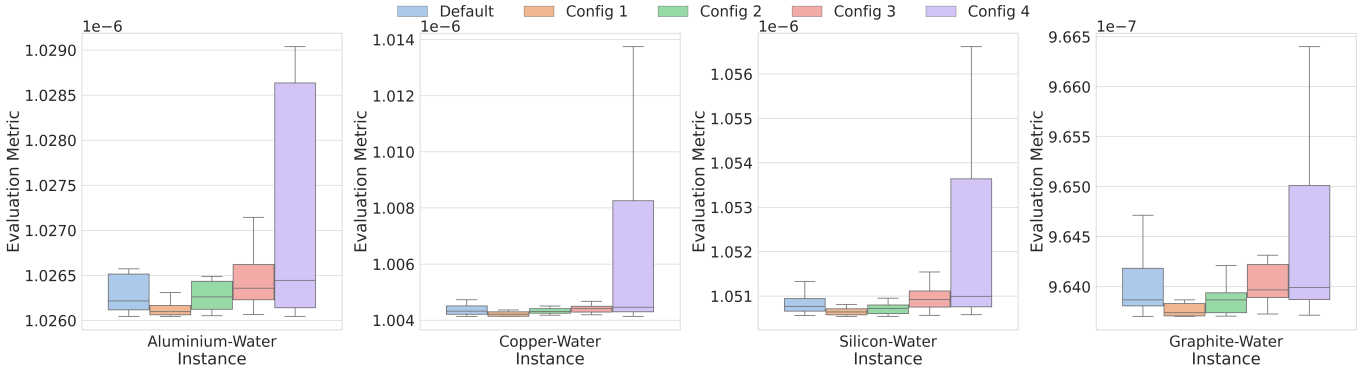

Fig. 2. Results achieved using the default collection of Search Operators.

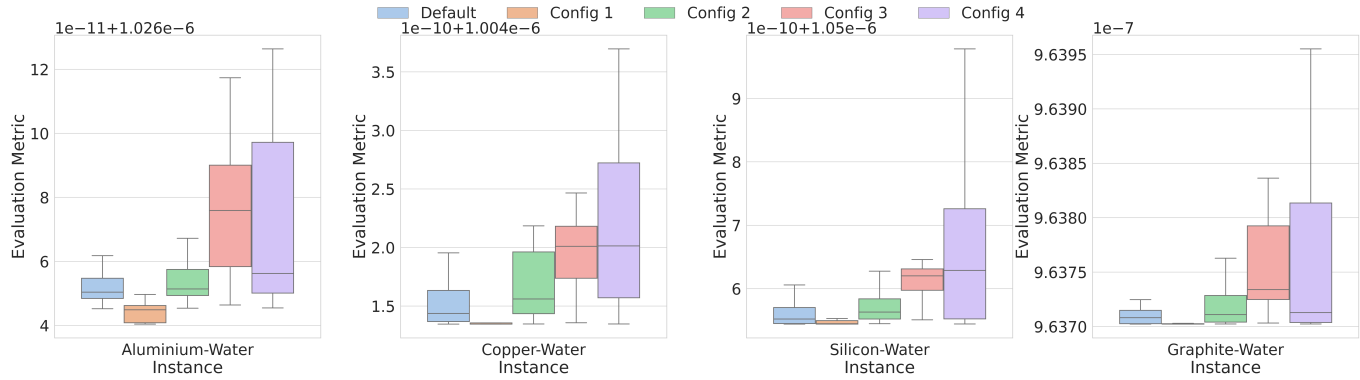

Fig. 3. Results achieved using the Collection 1 of Search Operators.

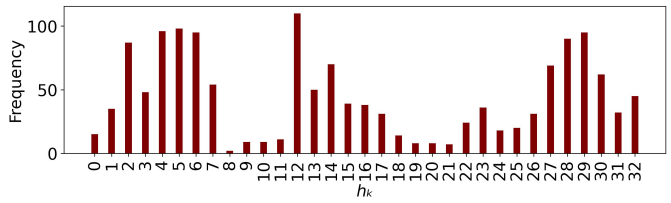

Fig. 4. Frequencies of the results from the second set of experiments.

ning with two Differential Mutation operators and concluding with one from the other two families. This finding provides valuable guidance for future research and underscores the significance of including such operators in a curated collection to tackle the problem effectively.

We then proceeded to the second phase of our experiments, focusing exclusively on the aluminum and water combination. Based on the results obtained, we selected the most effective configuration out of the five for each collection. Table VIII presents the chosen MHs and their configurations. MH_1 denotes the MH derived from the default collection's outcomes, MH_2 represents the best from Collection 1, and MH_3 from Collection 2. These selected MHs, along with seven other state-of-the-art MHs, were subjected to 100 iterations across 30 trials for each material-coolant pairing. The resulting entropy generation rate values were captured for analysis.

TABLE VIII
STRUCTURE OF THE MHS SELECTED FROM THE AL-H_2O COMBINATION GIVEN THEIR SEARCH OPERATORS ($\bar{h}_o$).

MH_k	Search Operators, $\bar{h}_o$	Collection size
MH_1	$(h_{DM} \circ h_g) \circ (h_{GC} \circ h_m) \circ (h_{CFD} \circ h_g)$	205
MH_2	$(h_{DM} \circ h_g) \circ (h_{DM} \circ h_g) \circ (h_{GC} \circ h_g)$	33
MH_3	$(h_{GC} \circ h_g) \circ (h_{DM} \circ h_g) \circ (h_{DM} \circ h_g)$	14

Using the gathered data, we performed a One-Sided Wilcoxon signed-rank test to ascertain whether there was statistical evidence to confirm our tailored MHs' superiority over state-of-the-art ones, setting $\alpha = 0.05$ as the threshold for rejecting the null hypothesis. The results of these tests are detailed in Tables IX and X. The p-values did not provide statistical evidence to assert that MH_1 outperforms the state-of-the-art MHs, as it displayed comparable or occasionally inferior results. Its performance was statistically better than DE only in the HTCG and Copper instances, with p-values lower than α. Interestingly, the results also indicated that MH_2 does not statistically surpass MH_1; however, MH_3 demonstrates a statistically significant improvement over both MH_1 and MH_2 in at least three of the four material instances, indicating a performance boost with the use of the curated collection. We

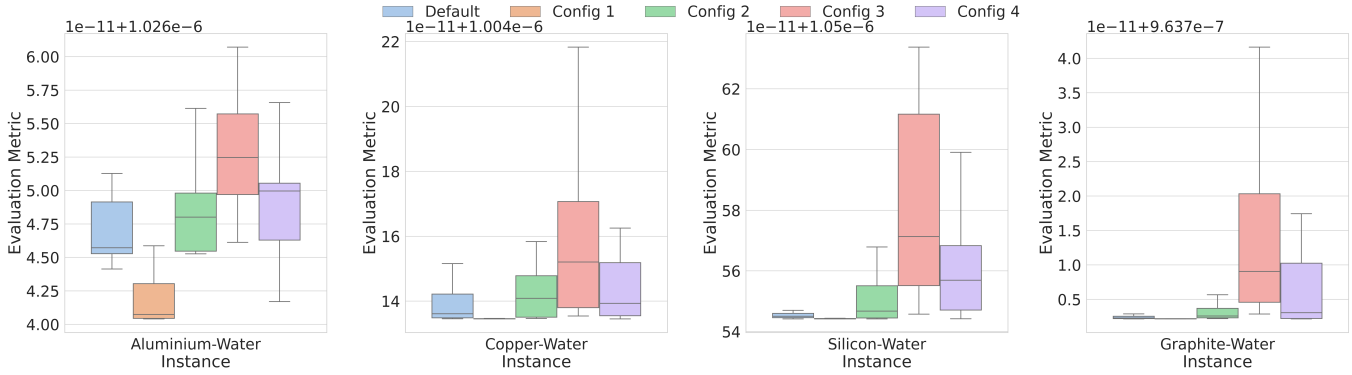

Fig. 5. Results achieved using the Collection 2 of Search Operators.

also proved that the filtration of the operators was done correctly. This enhancement is further corroborated by Table XI, which shows that MH_3, powered by the curated collection, is statistically superior to the state-of-the-art MHs, except for CS. The prevalence of p-values below the α level in most scenarios highlights the degree of improvement achieved with MH_3 compared to the initial MH_1 results.

TABLE IX
ONE-SIDED WILCOXON PAIR RANKED RESULTS FROM COMPARING MH_1 AGAINST THE STATE-OF-THE-ART MHS ($^*p < 0.05$, $^{**}p < 0.01$).

Mat.	p-value from comparing MH_1 vs.						
	RS	SA	DE	GA	PSO	CS	SD+GC
Si	0.99	0.99	0.08	0.99	0.74	1.00	0.91
HTCG	0.81	0.81	0.01*	0.81	0.11	1.00	0.06
Cu	0.68	0.68	0.01*	0.68	0.08	0.90	0.19
Al	0.66	0.95	0.04*	0.95	0.60	1.00	0.34

TABLE X
ONE-SIDED WILCOXON PAIR RANKED RESULTS FROM COMPARING THE SELECTED TAILORED MHS BETWEEN THEM ($^*p < 0.05$, $^{**}p < 0.01$).

Mat.	p-value from comparing		
	MH_2 vs MH_1	MH_3 vs MH_1	MH_3 vs MH_2
Si	0.1150	4.86×10^{-5}**	0.0062**
HTCG	0.1051	0.0015**	0.2929
Cu	0.8132	0.2024	0.0360*
Al	0.0693	0.0003**	0.0049**

Additionally, when adjusting for the true statistical significance across multiple pairwise comparisons as outlined in [28], the accumulated p-value supports the statistical superiority of MH_3 over most state-of-the-art MHs tested. While MH_3 does not uniformly outperform CS, a focused analysis on scenarios where MH_3 significantly outshines CS yields an accumulated p-value of 4.84×10^{-3}. This figure falls below our alpha threshold, affirming that MH_3 is substantially better than CS, particularly in the HTCG and aluminum cases. The outcomes

TABLE XI
ONE-SIDED WILCOXON PAIR RANKED RESULTS FROM COMPARING MH_3 AGAINST STATE-OF-THE-ART MHS ($^*p < 0.05$, $^{**}p < 0.01$).

Mat.	p-value from comparing MH_3 vs.						
	RS	SA	DE	GA	PSO	CS	SD+GC
	$\times10^{-3}$	$\times10^{-3}$	$\times10^{-5}$	$\times10^{-3}$	$\times10^{-5}$	$\times10^{-3}$	$\times10^{-5}$
Si	0.2**	0.2**	0.5**	0.2**	5.8**	336.6	4.9**
HTCG	0.2**	0.2**	2.4**	0.2**	4.9**	4.6**	0.7**
Cu	1.4**	1.4**	4.1**	1.4**	30.0**	60.0	50.0**
Al	0.1*	0.1*	0.1**	0.2**	4.9**	0.2**	3.5**

in the other two cases remain unchanged. These findings further accentuate the benefits and improved performance of a curated collection.

V. CONCLUSIONS

In this study, we employed an Automated Algorithm Design (AAD) strategy to develop Metaheuristics (MHs) tailored for Microelectronic Thermal Management scenarios, achieving performance comparable to or better than existing solutions in the literature. Additionally, we refined the heuristic space (metaheuristic parts) to facilitate and enhance the tailoring process. This approach successfully condensed the heuristic space, enabling the generation of more effective and consistent MHs compared to those using the standard configuration.

The tailored MHs from this curated space, which are population-based and metaphor-less, were statistically superior to traditional solvers such as PSO and GA. However, they only outperformed some state-of-the-art MHs. The results demonstrated the feasibility of using this approach to solve similar problems, enabling practitioners to find the proper solver without an extensive background in heuristic-based optimization. We recommend that researchers dealing with similar problem scenarios utilize the refined heuristic space to identify the most effective MH. Should this not meet the expected performance, the process we developed for curating the heuristic space can be reapplied to refine the collection further for the specific problem family.

Encouraged by these promising results, we are eager to extend our research and propose several avenues for future studies. Exploring alternative criteria for filtering operators could refine the precision of our metaheuristics. Additionally, while incorporating every possible operator is infeasible, testing this procedure with a diverse set of operators might further enrich our insights. Introducing new base materials and coolants into the microchannel heat sink design could also deepen our understanding of heuristic operators and the inherent characteristics of the problem. Conducting a study to map problem-domain features to heuristic spaces is essential for advancing our knowledge and application of these methods. Moreover, this study serves as a proof of concept for a methodology to enhance automated metaheuristic design. Future enhancements, such as expanding the range of search operator families and integrating the resulting metaheuristics into a hyper-parameter fine-tuning process, could further improve the overall effectiveness of this approach.

ACKNOWLEDGMENTS

This work was supported by the Research Group in Advanced Artificial Intelligence at Tecnológico de Monterrey, financially funded by Tecnológico de Monterrey under grants NUA A01172974, FAP 2570, and OPEX GIs 23-24, and by the Mexican Council of Humanities, Sciences, and Technologies (CONAHCyT) under scholarship 1151701.

REFERENCES

[1] H. E. Ahmed, B. Salman, A. Kherbeet, and M. Ahmed, "Optimization of thermal design of heat sinks: A review," *International Journal of Heat and Mass Transfer*, vol. 118, pp. 129–153, 2018.

[2] A. Moradikazerouni, "Heat transfer characteristics of thermal energy storage system using single and multi-phase cooled heat sinks: A review," *Journal of Energy Storage*, vol. 49, p. 104097, 2022.

[3] W. Li, Z. Xie, K. Xi, S. Xia, and Y. Ge, "Constructal optimization of rectangular microchannel heat sink with porous medium for entropy generation minimization," *Entropy*, vol. 23, no. 11, p. 1528, 2021.

[4] M. Mieczkowski, P. Furmański, and P. Łapka, "Optimization of a microchannel heat sink using entropy minimization and genetic aggregation algorithm," *Applied Thermal Engineering*, vol. 191, p. 116840, 2021.

[5] S. P. Adam, S.-A. N. Alexandropoulos, P. M. Pardalos, and M. N. Vrahatis, "No Free Lunch Theorem: A Review," in *Approximation and Optimization*, I. Demetriou and P. Pardalos, Eds. Cham: Springer, 2019, pp. 57–82.

[6] K. Sörensen, M. Sevaux, and F. Glover, "A history of metaheuristics," *Handbook of Heuristics*, vol. 2-2, pp. 791–808, 2018.

[7] A. A. Juan, P. Keenan, R. Martí, S. McGarraghy, J. Panadero, P. Carroll, and D. Oliva, "A review of the role of heuristics in stochastic optimisation: from metaheuristics to learnheuristics," *Ann. Oper. Res.*, vol. 320, pp. 831–861, jun 2021.

[8] K. Hussain, M. N. M. Salleh, S. Cheng, and Y. Shi, "Metaheuristic research: a comprehensive survey," *Artificial Intelligence Review*, vol. 52, no. 4, pp. 2191–2233, 2019.

[9] M. Sánchez, J. M. Cruz-Duarte, J. C. Ortiz-Bayliss, H. Ceballos, H. Terashima-Marin, and I. Amaya, "A systematic review of hyper-heuristics on combinatorial optimization problems," *IEEE Access*, vol. 8, pp. 128 068–128 095, 2020.

[10] J. M. Cruz-Duarte, I. Amaya, J. C. Ortiz-Bayliss, S. E. Conant-Pablos, H. Terashima-Marín, and Y. Shi, "Hyper-heuristics to customise metaheuristics for continuous optimisation," *Swarm and Evolutionary Computation*, vol. 66, p. 100935, 2021.

[11] J. M. Cruz-Duarte, J. C. Ortiz-Bayliss, I. Amaya, and N. Pillay, "Global optimisation through hyper-heuristics: Unfolding population-based metaheuristics," *Applied Sciences*, vol. 11, no. 12, p. 5620, jun 2021.

[12] R. Qu, G. Kendall, and N. Pillay, "The general combinatorial optimisation problem: Towards automated algorithm design," *IEEE Comp. Intel. Magazine*, vol. 15, no. 2, pp. 14–23, 2020.

[13] J. M. Cruz-Duarte, I. Amaya, J. C. Ortiz-Bayliss, and N. Pillay, "Automated design of unfolded metaheuristics and the effect of population size," in *2021 IEEE Congress on Evolutionary Computation (CEC)*. Kraków, Poland: Institute of Electrical and Electronics Engineers (IEEE), 2021, pp. 1155–1162.

[14] J. H. Drake, A. Kheiri, E. Özcan, and E. K. Burke, "Recent advances in selection hyper-heuristics," *European Journal of Operational Research*, vol. 285, no. 2, pp. 405–428, 9 2020.

[15] J. M. Cruz-Duarte, J. C. Ortiz-Bayliss, I. Amaya, Y. Shi, H. Terashima-Marín, and N. Pillay, "Towards a Generalised Metaheuristic Model for Continuous Optimisation Problems," *Mathematics*, vol. 8, no. 11, p. 2046, 2020.

[16] N. Pillay and R. Qu, *Hyper-Heuristics: Theory and Applications*. Cham: Springer, 2018.

[17] E. K. Burke, M. R. Hyde, G. Kendall, G. Ochoa, E. Özcan, and J. R. Woodward, "A classification of hyper-heuristic approaches: revisited," in *Handbook of Metaheuristics*. Cham: Springer, 2019, pp. 453–477.

[18] Z. He, Y. Yan, and Z. Zhang, "Thermal management and temperature uniformity enhancement of electronic devices by micro heat sinks: A review," *Energy*, vol. 216, p. 119223, 2021.

[19] M.-F. Chen, F.-C. Chen, W.-C. Chiou, and D. C. Yu, "System on integrated chips (soic(tm) for 3d heterogeneous integration," in *2019 IEEE 69th Electronic Components and Technology Conference (ECTC)*. Las Vegas, NV: Institute of Electrical and Electronics Engineers (IEEE), 2019, pp. 594–599.

[20] J. M. Cruz-Duarte, I. Amaya, J. C. Ortiz-Bayliss, and R. Correa, "Solving microelectronic thermal management problems using a generalized spiral optimization algorithm," *Applied Intelligence*, vol. 51, no. 8, pp. 5622–5643, 2021.

[21] W. A. Khan, M. M. Yovanovich, and J. R. Culham, "Optimization of microchannel heat sinks using entropy generation minimization method," in *Twenty-Second Annual IEEE Semiconductor Thermal Measurement And Management Symposium*. Dallas, TX: IEEE, 2006, pp. 78–86.

[22] A. M. Adham, N. Mohd-Ghazali, and R. Ahmad, "Optimization of an ammonia-cooled rectangular microchannel heat sink using multi-objective non-dominated sorting genetic algorithm (NSGA2)," *Heat Mass Transfer*, vol. 48, no. 10, pp. 1723–1733, may 2012.

[23] J. M. Cruz-Duarte, I. Martin-Diaz, J. U. Munoz-Minjares, L. A. Sanchez-Galindo, J. G. Avina-Cervantes, A. Garcia-Perez, and C. R. Correa-Cely, "Primary study on the stochastic spiral optimization algorithm," in *IEEE International Autumn Meeting on Power, Electronics and Computing*. Ixtapa, Mexico: IEEE, nov 2017, pp. 1–6.

[24] A. Bejan, "Entropy generation minimization: The new thermodynamics of finite-size devices and finite-time processes," *Journal of Applied Physics*, vol. 79, no. 3, pp. 1191–1218, 1996.

[25] T. L. Bergman, F. P. Incropera, D. P. DeWitt, and A. S. Lavine, *Fundamentals of heat and mass transfer*. Hoboken, N.J: John Wiley & Sons, 2011.

[26] S. G. Kandlikar, S. Colin, Y. Peles, S. Garimella, R. F. Pease, J. J. Brandner, and D. B. Tuckerman, "Heat Transfer in Microchannels–2012 Status and Research Needs," *Heat Transfer*, vol. 135, no. September 2013, p. 18, 2013.

[27] J. M. Cruz-Duarte, I. Amaya, J. C. Ortiz-Bayliss, H. Terashima-Marín, and Y. Shi, "CUSTOMHyS: Customising Optimisation Metaheuristics via Hyper-heuristic Search," *SoftwareX*, vol. 12, p. 100628, 2020.

[28] S. García, D. Molina, M. Lozano, and F. Herrera, "A study on the use of non-parametric tests for analyzing the evolutionary algorithms' behaviour: A case study on the cec'2005 special session on real parameter optimization," *J. Heuristics*, vol. 15, pp. 617–644, 12 2009.